ISSN 0006-2979, Biochemistry (Moscow), 2026, Vol. 91, No. 10, pp. 1922-1936 © Pleiades Publishing, Ltd., 2026.

Acridone Acetic Acid (CMA) Activates STING Signaling in Human Myeloid Leukemia Cells and Sensitizes Them to Venetoclax

Ivan A. Nevzorov[1#], Polina Korableva[1#], Oleg Shuvalov[1], Sergey Parfenyev[1], and Alexandra Daks[1,a*]

[1]*Institute of Cytology, Russian Academy of Sciences, 194064 Saint Petersburg, Russia*
[a]*e-mail: alexandra.daks@gmail.com*

Received June 1, 2026
Revised October 5, 2026
Accepted October 5, 2026

Abstract—The STING signaling pathway is a key regulatory mechanism of the innate immune response that coordinates the recognition of foreign double-stranded DNA molecules in the cytoplasm and participates in the regulation of numerous cellular processes associated with carcinogenesis. Modulation of this cascade is considered a promising approach to the treatment of infectious and autoimmune diseases, as well as various malignancies. By analyzing RNA-sequencing data, we demonstrated that STING/TMEM173 expression is elevated in acute myeloid leukemia cells and is an unfavorable prognostic factor for patients with this diagnosis. One potential STING agonist is 10-carboxymethyl-9-acridanone/acridone acetic acid (CMA), whose effect on this pathway has been demonstrated in murine cells, but not in human cells. CMA is an active component of immunostimulatory drugs registered in the Russian Federation. Analysis of the effects of CMA on KG-1 and K562 human myeloid leukemia cells demonstrated that CMA upregulated the expression of *STING*, *TBK1*, *IRF3*, *IRF7*, and STING-dependent inflammatory mediators, with this effect being most pronounced in K562 cells. According to the data obtained, CMA-treated K562 cells exhibited a more intense induction of genes regulating the mitochondrial apoptotic pathway. This finding was also consistent with a more pronounced decrease in the viability of K562 cells compared with KG-1 cells treated with CMA. Analysis of combinations with antitumor drugs showed that CMA antagonized the cytotoxic activity of doxorubicin and cisplatin, but exhibited pronounced synergy when combined with the Bcl-2 inhibitor venetoclax. The obtained data indicate that CMA can be considered a potential STING agonist in human cells in vitro at high concentrations; however, its therapeutic potential, molecular mechanisms of action, efficacy, and safety require careful preclinical and clinical evaluation.

DOI: 10.1134/S0006297926601772

Keywords: cGAS-STING signaling pathway, STING agonist, acridone acetic acid (CMA), acute myeloid leukemia (AML), synergy, venetoclax, innate immunity, type I interferon, combined antitumor therapy, apoptosis

INTRODUCTION

The STING signaling pathway is one of the key regulatory mechanisms of the innate immune response, coordinating recognition of the double-stranded DNA molecules in the cytoplasm and their elimination. Upon entering the cytoplasm, the foreign DNA, mitochondrial DNA, or DNA released upon the death of surrounding cells binds to the cyclic GMP-AMP synthase (cGAS), an enzyme catalyzing synthesis of the second messenger 2′3′-cyclic GMP-AMP (2′3′-cGAMP). The synthesized 2′3′-cGAMP activates the endoplasmic reticulum (ER) resident protein STING, encoded by the gene *STING* (*TMEM173*), which, upon binding 2′3′-cGAMP, translocates to the ER-Golgi intermediate compartment (ERGIC), where it recruits and activates the kinase TBK1. The TBK1 activation causes trans-autophosphorylation of this enzyme at the serine residue at position 172 (Ser172) [1, 2], as well as phosphory-

* To whom correspondence should be addressed.
# These authors contributed equally to this study.

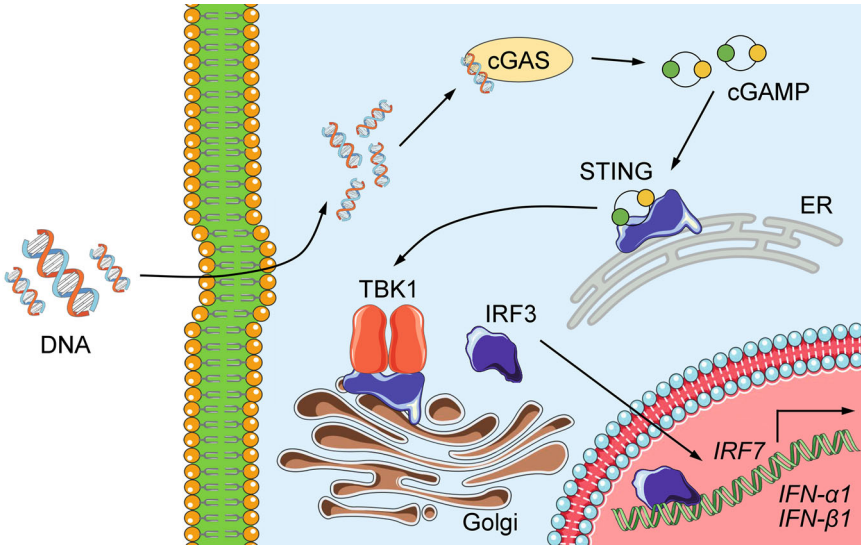

Fig. 1. Scheme of the canonical activation pathway of the STING signaling cascade. Upon entering the cell cytoplasm, foreign DNA is detected by the cGAS protein, which, in turn, begins synthesis of the cyclic dinucleotide cGAMP. cGAMP binds to the protein STING, which leads to its detachment from the endoplasmic reticulum (ER) membrane and its transfer to the Golgi apparatus (GA), where it is recruited by the protein TBK1, forms a complex with it, and is phosphorylated. This complex then recruits the transcription factor IRF3, phosphorylating it. The phosphorylated IRF3 enters the nucleus and triggers expression of the transcription factor IRF7 and type I interferons, activating the cellular immune response.

lation of STING (at Ser366) [3] and of the transcription factor IRF3 (at Ser396, Ser398, Ser402, Thr404, Ser405) [4]. The IRF3 phosphorylation results in its dimerization and translocation to the nucleus, where it induces expression of the type I interferons (IFN1) and IRF7, which, in turn, activate the IFN-stimulated genes (ISGs) such as *IFIT1-3*, *MX1*, *OAS1*, *CXCL9-11*, as well as certain interleukins (e.g., *IL1B* and *IL6*) [5, 6]. An important feature of the STING signaling pathway is its ability to positively regulate expression of not only pro-inflammatory but also pro-apoptotic genes, such as *BAX* and *NOXA*; however, the mechanisms regulating this "switch" remain insufficiently studied to date (Fig. 1).

Dysfunction of the STING-dependent signaling is associated with a wide range of diseases and pathological conditions. Many viruses have been shown to suppress STING activation in infected cells through various molecular mechanisms. In particular, the membrane protein NS4B of the yellow fever virus, dengue virus, and hepatitis C virus, belonging to the family *Flaviviridae*, cleaves the STING protein in human cells and prevents activation of the interferon response [7, 8]. The tegument protein ORF52 of the Kaposi's sarcoma-associated herpesvirus type 8 and Epstein–Barr virus (family *Herpesviridae*) inhibits STING signaling by binding to cGAS and inhibiting it, which leads to the decreased level of cGAMP and, accordingly, suppression of the innate immune response upon infection [9]. Conversely, pathogenesis of a number of autoimmune diseases is accompanied by the increased level of STING signaling activity. To date, two diseases caused by the gain-of-function (GOF) mutations in the *STING* gene encoding the STING protein are known: the STING-associated vasculopathy with onset in infancy (SAVI syndrome) and certain forms of familial chilblain lupus [10]. Progression of other autoimmune diseases is often associated with accumulation of the cytoplasmic double-stranded DNA, which, in turn, could lead to hyperactivation of the STING cascade and type I interferonopathy, as in systemic lupus erythematosus and Aicardi–Goutières syndrome [11, 12].

In recent years, increasing attention has been paid to the role of the STING signaling cascade in carcinogenesis. Although dysfunction of this molecular pathway could be associated both with activation of the tumor formation through the maintenance of chronic inflammation and with suppression of the tumor progression, within the current paradigm STING signaling is considered one of the most important mechanisms underlying antitumor immunity [5]. Thus, it has been shown that the interferon response – a key process in T lymphocyte priming during carcinogenesis – directly depends on the cGAS-STING pathway, and *in vivo* experiments have shown that the tumor cell DNA is successfully recognized by cGAS and eliminated via the STING signaling cascade [13, 14]. Indeed, a number of studies demonstrate that activation of the STING signaling could promote a shift of the tumor immune phenotype from "cold" with low immunogenicity to "hot", characterized by active processes of the antitumor immune response [15, 16]. The oncosuppressive role of STING signaling

is confirmed by numerous clinical trials of the STING agonists, such as IMSA101, GSK3745417, MK-1454, and TAK-676, both as monotherapy and in combination with other antitumor drugs in the groups of patients with various types of malignant diseases [5].

One potential STING agonist is acridone acetic acid (10-carboxymethyl-9-acridone, CMA). In 1976, antiviral effect of this compound was first described in the mouse models of infection with Coxsackie viruses, herpes simplex, pseudorabies, western equine encephalitis, and others [17]. Later, it was established that the antiviral action of CMA is based on activation of the type I interferon response [18]. In 2011, it was shown that CMA stimulates the STING signaling cascade due to its ability to bind to the nucleotide-binding domain of the STING protein. However, these data were obtained and confirmed by other researchers in murine cells, while in the studies with human cells CMA did not exert an interferon-stimulating effect [19]. Importantly, despite the obvious lack of large randomized clinical studies of the efficacy and specificity of CMA and poor understanding of the molecular mechanisms of its action in human cells, a derivative of this compound, meglumine acridone acetate, is an approved drug in Russia and is included in the Russian list of essential and vital medicines. Meglumine acridone acetate is an active component of such immunomodulatory drugs as Cycloferon and Neovir, recommended for treating influenza, acute respiratory viral infections, and infections caused by herpes viruses, HPV, HIV, etc.

In this work, we analyzed the pro-inflammatory and cytotoxic effects of CMA on the human myeloid leukemia cells and investigated the combined effect of CMA and antitumor drugs.

MATERIALS AND METHODS

Bioinformatic analysis. Analysis of the expression of *STING* and *IRF3* genes in the samples of normal and tumor tissues obtained from the patients was carried out using the freely available RNA sequencing databases (The Cancer Genome Atlas Program (TCGA), Genotype-Tissue Expression (GTEx), and Gene Expression Omnibus (GEO)) with the resources TNMplot V2 [20] and the web server GEPIA [21]. The correlation between the expression levels of the *STING* and *IRF3* genes and survival of the acute myeloid leukemia (AML) patients was determined using the GEO database and the Kaplan–Meier plotter resource [22]. Comparative analysis of the *STING* and *IRF3* gene expression in the tissue-specific groups of human cell lines was carried out using the Cell line resource of the Human Protein Atlas project [23].

Cell culturing. Myeloid leukemia cell lines K562 and KG-1 were kindly provided by the Core Shared Research Facility “Collection of Vertebrate Cell Cultures” (CSRF CVCC) of the Institute of Cytology, Russian Academy of Sciences (Saint Petersburg, Russia) and were cultured at 37°C in a 5% CO_2 atmosphere in a Roswell Park Memorial Institute (RPMI) 1640 medium (PanEco, Russia) supplemented with fetal bovine serum (FBS) (Gibco, USA) at the concentration of 10% and gentamicin at the concentration of 50 μg/ml. Cells at passages from 3 to 7 were used in the experiments.

MTT assay. 24 h before the start of an experiment, cells were seeded into 96-well culture plates 24 h before treatment with CMA, doxorubicin, cisplatin, or venetoclax at the indicated concentrations. 48 h after the start of treatment, 10 μl of a 5 mg/ml solution of 3-(4,5-dimethylthiazol-2-yl)-2,5-diphenyltetrazolium bromide (MTT) (Dia-M, Russia) was added to each well, and the plates were placed in a CO_2 incubator for 4 h. The plates were next centrifuged at 1500*g* for 10 min using an LMC-3000 plate centrifuge (BIOSAN, Latvia). The medium was then removed, 100 μl of DMSO was added to each well, and the plates were incubated with constant shaking for 30 min. Optical density of the solution was measured at wavelengths of 570 and 630 nm using an iMark plate spectrophotometer (Bio-Rad, USA). Cell viability was calculated as a relative value, taking optical density of the solution in the wells with control untreated cells as 100%. All experiments were performed in three biological replicates, each of which included 6 technical replicates for each experimental concentration. IC50 values were calculated by fitting the concentration–response data to a three-parameter inhibition model with the Hill slope fixed at −1.

Synergy analysis. Interactions between the studied compounds were assessed using the Loewe Additivity model, implemented with the SynergyFinder 3.0 tool [24]. For each point of the dose-response matrix, the expected additive effect y_Loewe was calculated from the following equation (1):

$$dA/fA^{-1}(y) + dB/fB^{-1}(y) = 1,$$

where dA and dB are concentrations of substances A and B in the combination; $fA^{-1}(y)$ and $fB^{-1}(y)$ are concentrations of each of the substances when used separately that are required to achieve the effect y according to the individual dose-response curves. The dose-response curves for each substance were fitted using a four-parameter logistic (4PL) model.

The degree of deviation of the observed effect from the expected additive effect was expressed using the synergy score (SS):

$$SS = y_observed - y_Loewe,$$

Table 1. Primers used for RT-PCR

Gene	Primer	Sequence
BAD	forward	GAGTGAGCAGGAAGACTCCAGC
BAD	reverse	TCCACAAACTCCTCACTCATCC
BAK1	forward	GGGTGTAGATGGGGGAACTGTG
BAK1	reverse	AACACCCTAGGCTGTGCCCAAT
BAX	forward	CAGCTCTGAGCAGATCATGAAGACA
BAX	reverse	GCCCATCTTCTTCCAGATGGTGAGC
BBC3	forward	GCGAGACTGTGGCCTTGTGT
BBC3	reverse	CGTTCCAGGGTCCACCAAAGT
BCL-XL	forward	GCCACTTACCTGAATGACCACC
BCL-XL	reverse	AACCAGCGGTTGAAGCGTTCCT
BCL2	forward	CCGCATCAGGGAAGGCTAGAG
BCL2	reverse	CTGGGACACAGGCAGGTTCT
GAPDH	forward	GTCTCCTCTGACTTCAACAGCG
GAPDH	reverse	ACCACCCTGTTGCTGTAGCCAA
IFNB1	forward	ACGCCGCATTGACCATCTAT
IFNB1	reverse	GTCTCATTCCAGGTCACGCT
IL1B	forward	ATCCCCAGCCCTTTTGTTGA
IL1B	reverse	TTTCTGTCAGGCGGGCTTTA
IL6	forward	GACCCAACCACAAATGCCAG
IL6	reverse	GTGCCCATGCTACATTTGCC
IRF3	forward	CACATTTCCAACAGCCACCC
IRF3	reverse	GTAGGCCTTGTACTGGTCGG
IRF7	forward	GCTGGACGTGACCATCATGTA
IRF7	reverse	GGGCCGTATAGGAACGTGC
MCL1	forward	GCTGGGATGGGTTTGTGGAG
MCL1	reverse	TTTGGTGGTGGTGGTGGTTG
NOXA	forward	CTGGAAGTCGAGTGTGCTACTC
NOXA	reverse	TGAAGGAGTCCCCTCATGCAAG
STING	forward	CCTGAGTCTCAGAACAACTGCC
STING	reverse	GGTCTTCAAGCTGCCCACAGTA
TBK1	forward	TGATCTTTGGAGCATTGGGGT
TBK1	reverse	AGGGTCTAAATGGCAGTGATCC

where positive SS values indicate synergism (the observed effect exceeds the expected additive effect), and negative values indicate antagonism. According to the threshold criteria adopted in the SynergyFinder, SS values between −10 and +10 indicate an additive interaction; values above +10 indicate synergism, whereas values below −10 indicate antagonism. GraphPad Prism 8 software was used to construct heatmaps.

RNA isolation and quantitative real-time RT-PCR. Total RNA was isolated from cells using an ExtractRNA reagent (Evrogen, Russia) according to the manufacturer's instructions. Reverse transcription reaction was carried out using an oligo(dT) primer and a MMLV RT first-strand cDNA synthesis kit (Evrogen, Russia). The amount of RNA per reaction was 2 μg. To analyze gene expression using real-time PCR, a qPCRmix-HS SYBR reagent (Evrogen, Russia) and primers listed in Table 1 were used. Amplification was performed with a CFX96 Touch Real-Time PCR Detection System (Bio-Rad). The data were analyzed using the CFX Manager software. Messenger ribonucleic acid (mRNA) expression levels were calculated relative to the reference gene (GAPDH) by the $2^{-\Delta\Delta Ct}$ method. The number of biological replicates was 3, and the number of technical replicates was 3. One-way analysis of variance (ANOVA) was performed to assess statistical differences between the groups.

Statistical analysis. Relative change in gene expression levels in the real-time PCR method was assessed using the $2^{-\Delta\Delta Ct}$ algorithm. For the MTT assay and enzyme-linked immunosorbent assay (ELISA), mean values and standard error of the mean (SEM) were determined. One-way analysis of variance (ANOVA) was performed to determine statistical differences between the groups; p values are denoted as * $p < 0.05$.

PAGE and Western blotting. For Western blot analysis, cell extracts were prepared using a radioimmunoprecipitation (RIPA) buffer. For polyacrylamide gel electrophoresis (PAGE), Laemmli buffer was added to the cell extracts, followed by denaturation at 97°C for 5 min. After PAGE electrophoresis, the proteins were transferred to a polyvinylidene fluoride membrane using a Trans-Blot Turbo system (Bio-Rad). Protein transfer was carried out in a Tris-glycine buffer (TGB) containing 20% ethanol for 1.5 h at 100 V and 4°C. The following primary antibodies were used: anti-β-actin (Sigma-Aldrich, USA), anti-α-tubulin (Sigma-Aldrich), anti-cGAS, anti-STING, anti-p-STING (Ser366), anti-TBK1, anti-p-TBK1 (Ser172), anti-IRF3 and anti-p-IRF3 (Ser396) (Affinity, Canada), anti-Bax (Cell Signaling), anti-Bcl-2 (Cell Signaling). Anti-mouse IgG and anti-rabbit IgG secondary antibodies (1 : 10,000; Sigma-Aldrich) were used. Chemiluminescent signals were detected using a Clarity™ Western ECL substrate (Bio-Rad) and a ChemiDoc MP imaging system (Bio-Rad). The number of biological replicates was 3.

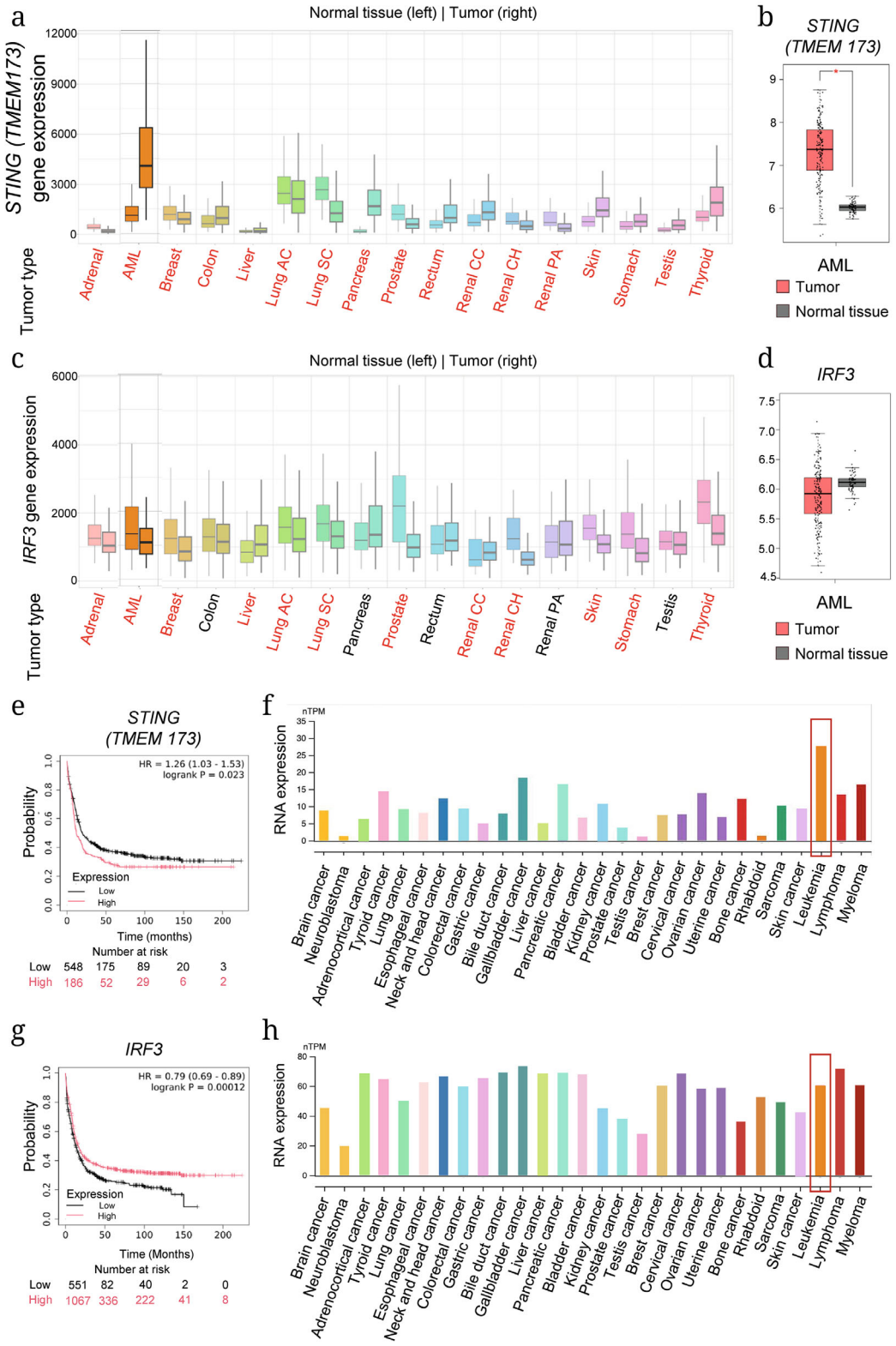

Fig. 2. Expression patterns and prognostic significance of the *STING* (*TMEM173*) and *IRF3* expression levels in AML and other malignancies. Analysis of *STING* (*TMEM173*) (a) and *IRF3* (c) expression in tumor and normal tissues using TNMplot; tissue types in which the difference in the expression of the studied genes between the tumor and normal tissues is statistically significant are highlighted in red; results of differential expression analysis of *STING* (*TMEM173*) (b) and *IRF3* (d) in AML using GEPIA; expression in the tumor tissues is marked in red, and in normal tissues in black; analysis of correlation of the expression level of *STING* (*TMEM173*) (e) and *IRF3* (g) with survival of the AML patients using Kaplan–Meier Plotter; assessment of the expression levels of the genes *STING* (*TMEM173*) (f) and *IRF3* (h) in various groups of cell lines based on Human Protein Atlas data.

RESULTS

Bioinformatic analysis of *STING* and *IRF3* expression in human cancer cells. According to numerous reports, as well as data obtained by our research group, altered STING signaling is characteristic of various types of solid and hematological malignancies [5, 6, 25]. At the first stage, using the TNMplot resource, we analyzed differences in the expression of the key participants of the STING signaling cascade – the adaptor factor STING itself (the gene *STING*, also known as *TMEM173*) and the transcription factor IRF3. Figure 2 demonstrates a list of malignancies in which significant differences in the *STING* expression between the tumor and non-tumor tissues are observed. Notably, depending on the tumor type, STING expression was either higher or lower in tumor tissues than in the corresponding normal tissues (Fig. 2a). For example, the *STING* level is elevated in the intestinal, pancreatic, and skin cancer samples and decreased in the lung, breast, and adrenal cancer compared to the samples of the corresponding non-transformed tissues. Of particular note is the pronounced increase in the expression level of this gene in the AML samples. Meanwhile, analysis of the *IRF3* gene expression level revealed not an increase, but a significant decrease in the AML samples compared to the samples obtained from the healthy donors (Fig. 2c). We confirmed the increased expression of the *STING* gene in the AML samples by differential expression analysis using the GEPIA platform (Fig. 2b). For the *IRF3* gene, a tendency toward decreased expression in tumor cells was also observed, but no significant differences were found (Fig. 2d).

At the next stage, correlation of the expression levels of the *STING* and *IRF3* genes with survival of the AML patients was assessed. The analysis was performed using the publicly available gene expression microarray data from the GEO repository and the Kaplan-Meier Plotter resource. As a result, we found that a high level of *STING* expression is significantly associated with the less favorable survival prognosis for the AML patients (Fig. 2e), whereas high level of *IRF3* expression, on the contrary, is a favorable prognostic marker (Fig. 2g). These results are consistent with the data on the differential expression of the *STING* and *IRF3* genes in the AML samples and samples from healthy donors but raise an important question about the biological effect of modulating the STING signaling cascade in this diagnosis. Moreover, analysis of the expression levels of *STING* and *IRF3* in various groups of cell lines showed that in the hematological tumors, and, in particular, in the myeloid leukemia cells, high levels of *STING* and *IRF3* expression are observed (Fig. 2, f and h).

Thus, taking into account the data of our bioinformatic analysis, we hypothesized that the potential STING agonist may influence activity of the STING signaling cascade in the human myeloid leukemia cells and their susceptibility to chemotherapy.

CMA activates expression of the STING-dependent innate immunity factors in the human myeloid leukemia cells. The KG-1 and K562 lines were chosen as model myeloid leukemia cell lines. Analysis of basal STING, TBK1, IRF3, and IRF7 expression showed that KG-1 cells had higher expression levels of STING, TBK1, and IRF7, whereas K562 cells had higher IRF3 expression (Fig. 3).

Analysis of the expression levels of mRNAs of the key participants of the STING cascade in KG-1 and K562 cells treated with 1- and 4-mM CMA for 16 h showed that in K562 cells there was a significant in-

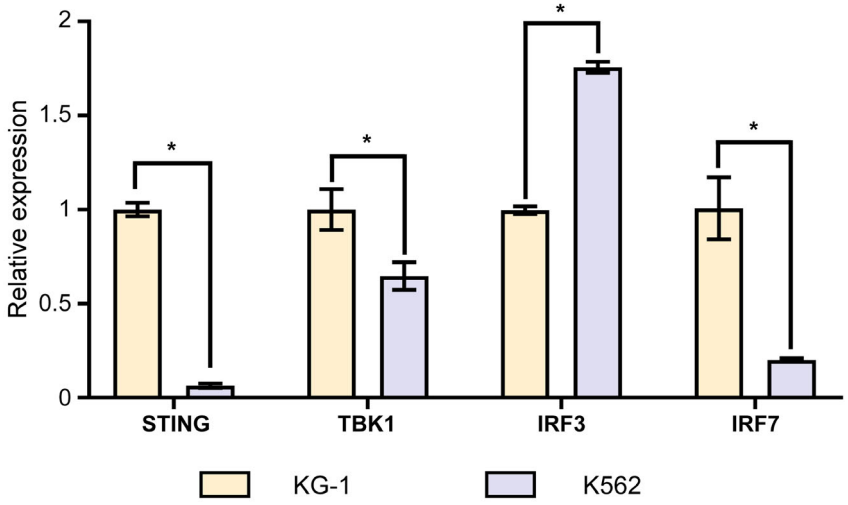

Fig. 3. Basal expression level of the STING signaling cascade genes in the KG-1 and K562 cell lines. Expression level of the studied gene in KG-1 cells was taken as one. One-way analysis of variance (ANOVA) was performed to determine statistical differences between the groups; p values are denoted as * $p < 0.05$.

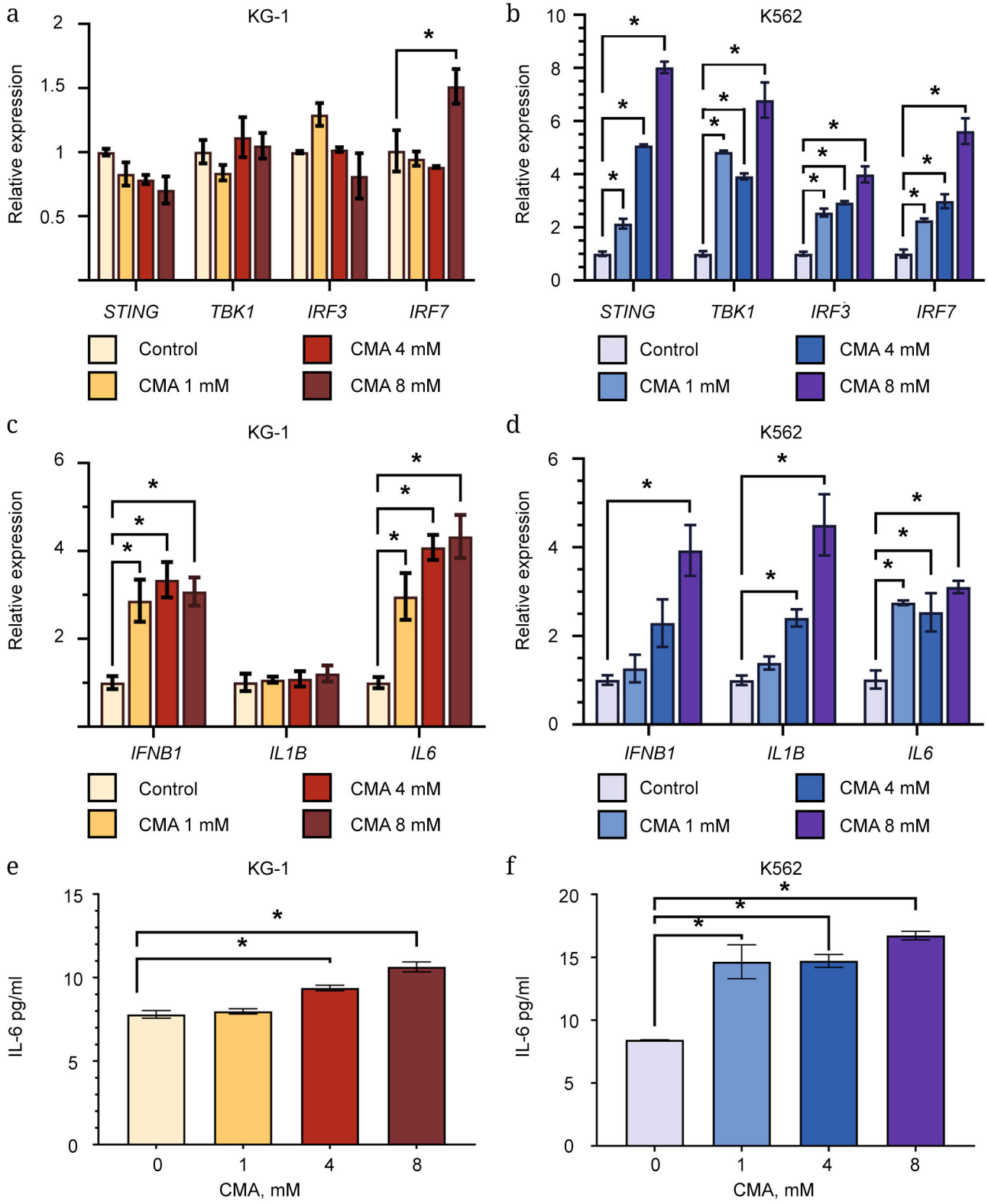

Fig. 4. Effect of CMA on activation of the STING signaling cascade in AML cells. a-d: Analysis of the expression of STING signaling cascade genes (a, b) and STING-dependent interferons and interleukins (c, d) in the KG-1 (a, c) and K562 (b, d) cell lines, performed using quantitative RT-PCR. Expression level of the studied gene in the control sample was taken as one. One-way analysis of variance (ANOVA) was performed to determine statistical differences between the groups; the p values are labelled as * $p < 0.05$; e and f: ELISA results demonstrating the level of IL-6 protein in the KG-1 (e) and K562 (f) AML cells treated with CMA for 16 h. One-way analysis of variance (ANOVA) was performed to determine statistical differences between the groups; the p values are labelled as * $p < 0.05$.

crease in the expression of the genes encoding STING, TBK1, IRF3, and IRF7 (Fig. 4b), while in KG-1 cells no significant change in the expression of these genes was detected (Fig. 4a).

It is known that expression of the innate immunity factors – type I interferon *IFNB1* and interleukins *IL1B* and *IL6* – is regulated by the STING signaling cascade and is activated by it in response to the stimuli such as entry of foreign nucleic acids into the cell cytoplasm or DNA released from the destroyed neighboring cells, due to mitochondrial damage, ER stress, etc. We analyzed expression of the *IFNB1*, *IL1B*, and *IL6* genes in KG-1 and K562 cells treated with CMA and showed that in the K562 line expression of all three of these genes increases with increasing CMA concentration (Fig. 4, b and d). In contrast to K562 cells, in KG-1 cells we observed increased expression of only *IFNB1* and *IL6*, but not of *IL1B* (Fig. 4, a and c).

To confirm activation of the STING signaling cascade in response to CMA treatment, an ELISA was performed; increase in the IL-6 level in AML cells treated with CMA for 16 h was demonstrated, which also indicated activation of the signaling cascade (Fig. 4, e and f). Notably, increase in the IL-6 concentration is more pronounced in K562 cells (about 2-fold) compared to KG-1 cells (not exceeding 1.4-fold), which is consistent with the quantitative RT-PCR data showing more significant activation of the STING signaling components in the K562 cell line in response to CMA treatment.

Additionally, the levels of the proteins STING, TBK1, and IRF3 involved in this signaling pathway, as well as their active phosphorylated forms, were analyzed upon CMA treatment for 3 h using Western blotting (Online Resource 1). Consequently, we observed increase in the levels of phosphorylated forms of the STING, TBK1, and IRF3 proteins in both cell lines. However, in KG-1 cells, the levels of pIRF3 and pSTING decreased at the maximum studied CMA concentration of 8 mM, whereas for K562 cells a steady increase in the level of the active forms of these proteins was observed with increasing CMA concentration. The observed effect of CMA is consistent with the RT-PCR results demonstrating lower level of activation of the pro-inflammatory response in KG-1 cells, as well as with the data previously published by us and other researchers [6, 26] on the wavelike character of the STING cascade activation.

Study of the effect of CMA on viability of the human myeloid leukemia cells and expression of apoptosis markers. At the next stage, we investigated the effect of various CMA concentrations on viability of KG-1 and K562 cells. Using the MTT assay, we determined half-maximal inhibitory concentrations (IC50) of CMA for the KG-1 and K562 cells, which amounted to 11.6 ± 1.15 mM for KG-1 and 8.5 ± 1.65 mM for K562 (Fig. 5, a and b).

Since it has previously been shown by us and other researchers that the alternative pathway of STING signaling activation could regulate expression of the genes associated with the process of apoptosis, in particular the genes of the Bcl-2 family [6, 27], we analyzed the effect of CMA on the expression level of the pro-apoptotic genes *BAK1* (BAK), *BBC3* (PUMA), *BAX*, *BAD*, and *NOXA*, as well as of the anti-apoptotic genes *BCL2* (Bcl-2), *BCL-XL*, and *MCL1* in both cell lines. Based on the determined IC50 values, the following CMA concentrations were chosen: 1, 4, and 8 mM for K562 and 1, 6, and 12 mM for KG-1. As a result, we showed that in the K562 cell line the levels of expression of all studied apoptosis-regulating genes increased with the increasing CMA concentration (Fig. 5d). In contrast, a much less pronounced change in the expression of the apoptosis-associated genes in response to CMA was observed in KG-1 cells, and the greatest increase upon treatment with 12 mM CMA was observed for the anti-apoptotic gene *BCL2*, which is consistent with the MTT data showing higher resistance of this cell line to CMA (Fig. 5b).

We also performed Western blot analysis to assess changes in the levels of the apoptosis factors Bax and Bcl-2 in both cell lines in response to the treatment with the indicated CMA concentrations for 16 h (Fig. 5, e and f). We found that the level of the pro-apoptotic protein Bax increased significantly in both K562 and KG-1 upon treatment with 1- and 4-mM CMA, whereas maximum level of the anti-apoptotic factor Bcl-2 was detected in both cell lines at the maximum CMA concentration (12 mM for KG-1 and 8 mM for K562) (Fig. 5f).

Exposure to CMA increases resistance of the KG-1 and K562 cell lines to doxorubicin and cisplatin but sensitizes them to the action of venetoclax. Based on the obtained data, we hypothesized that the combined use of CMA with antitumor drugs widely used in clinical practice could enhance their effect. As chemotherapeutic drugs inducing apoptosis in cancer cells, doxorubicin, which causes double-strand DNA breaks by inhibiting topoisomerase II [28], cisplatin, which causes formation of interstrand DNA crosslinks [29], and venetoclax, the selective inhibitor of the anti-apoptotic protein Bcl-2 [30], were chosen. To determine sensitivity of the KG-1 and K562 cell lines to the selected antitumor drugs both as single-agent treatment and in combination with treatment with various CMA concentrations, an MTT analysis was performed.

According to our results, both cell lines acquire resistance to doxorubicin and cisplatin in the presence of CMA (Fig. 6, a, c, e, g). The antagonistic effect of the combination of CMA with both doxorubicin

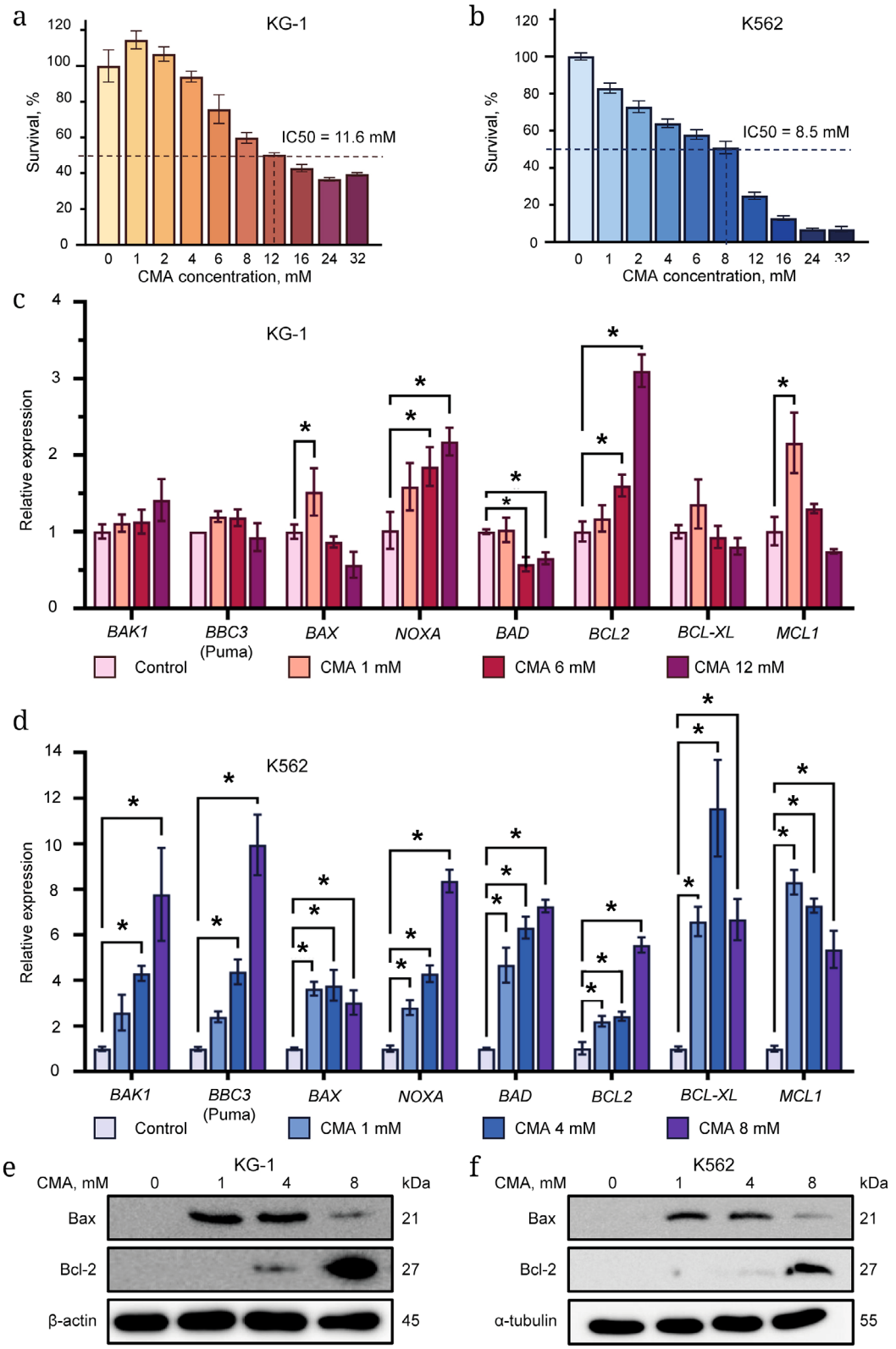

Fig. 5. Analysis of viability of the AML cells upon CMA treatment. MTT analysis of survival of the AML cell lines KG-1 (a) and K562 (b) upon CMA treatment; the dashed line indicates IC50 concentration and the corresponding survival; quantitative RT-PCR analysis of the expression of apoptosis regulator genes upon CMA treatment of AML cells KG-1 (c) and K562 (d) for 16 h. Expression level of the studied gene in the untreated control sample was taken as one. One-way analysis of variance (ANOVA) was performed to determine statistical differences between the groups; p values are denoted as * $p < 0.05$. Results of Western blot analysis of the expression levels of the proteins Bax and Bcl-2 in AML cells treated with CMA: KG-1 (e), K562 (f) for 16 h.

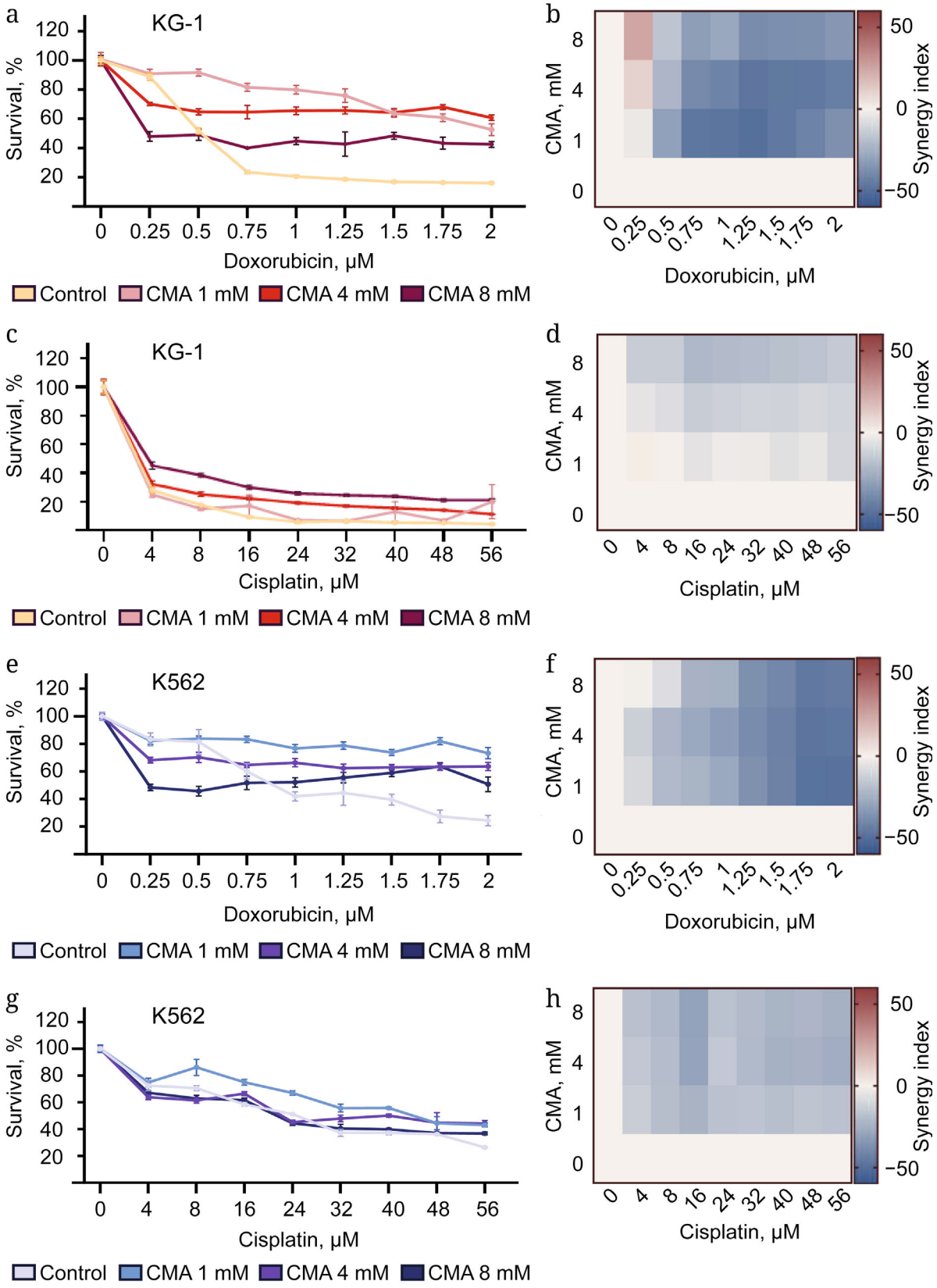

Fig. 6. Combined effect of CMA and doxorubicin or cisplatin on AML cell lines. MTT analysis of the survival of AML cell lines (KG-1 (a, c) and K562 (e, g)) treated with combination of CMA with doxorubicin (a, e) and cisplatin (c, g); heatmaps of the synergy index of CMA and doxorubicin (b, f) or cisplatin (d, h) upon treatment of the AML cell lines KG-1 (b, d) and K562 (f, h). The synergy index was calculated using the Loewe model. Red and blue colors denote positive and negative synergy index values, indicating the observed synergistic and antagonistic effects, respectively.

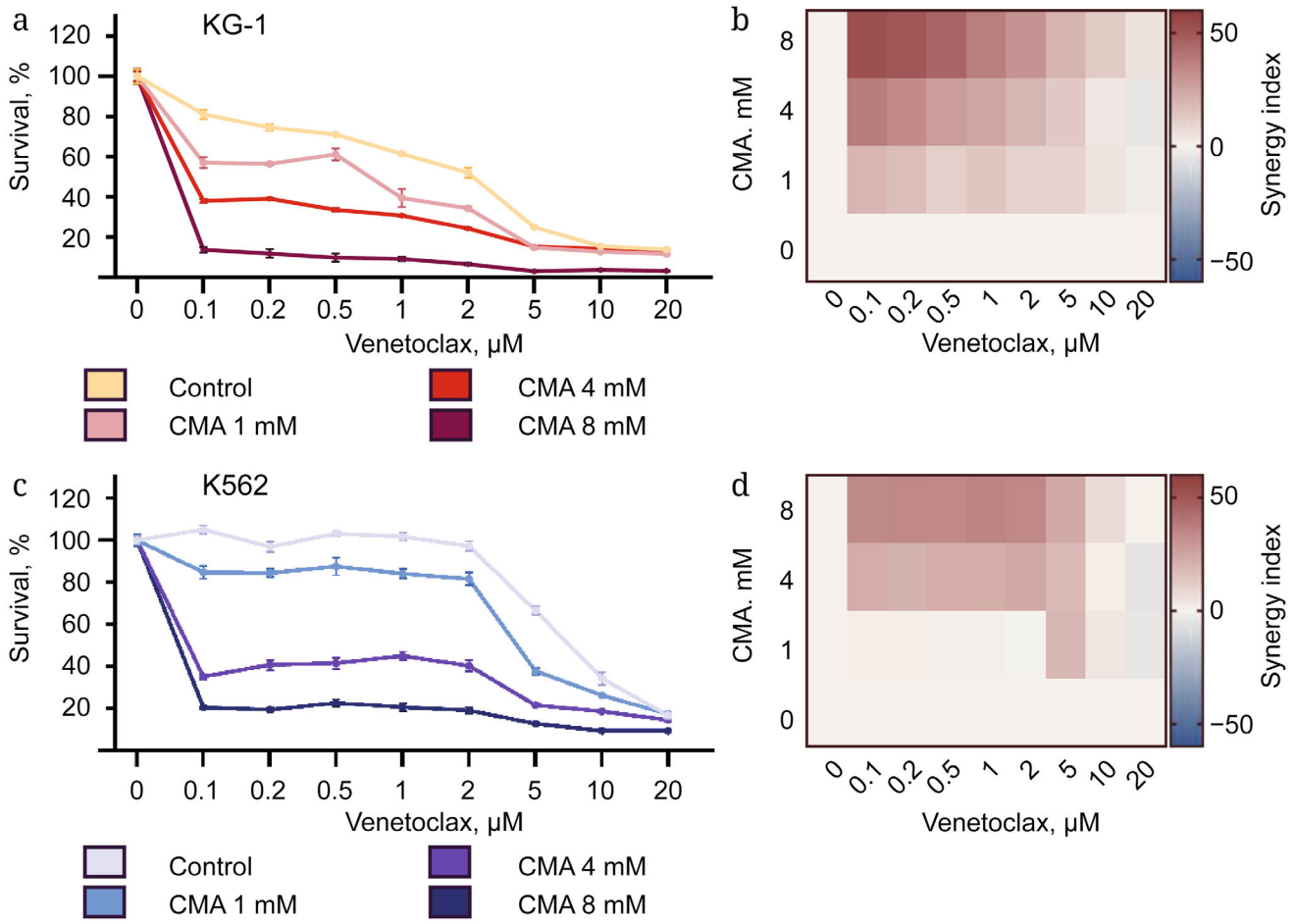

Fig. 7. Combined effect of CMA and venetoclax on AML cell lines. MTT analysis of survival of the KG-1 cell line upon combined treatment with CMA and venetoclax (a); heatmap of the synergy index of CMA and venetoclax upon treatment of the KG-1 cell line (b); MTT analysis of survival of the K562 cell line upon combined treatment with CMA and venetoclax (c); heatmap of the synergy index of CMA and venetoclax upon treatment of the K562 cell line (d). Synergy index was calculated using the Loewe model. Red and blue colors denote positive and negative synergy index values, indicating the observed synergistic and antagonistic effects, respectively.

and cisplatin is confirmed by the synergy analysis using the Loewe model, the results of which are shown in Fig. 6, b, d, f, h. Blue color in the heatmaps corresponds to the negative synergy index values, indicating the observed antagonistic effect.

However, when studying the combined action of CMA with venetoclax, we observed the opposite effect. Indeed, the combination of CMA and venetoclax exerts a pronounced synergistic effect on both myeloid leukemia cell lines (Fig. 7, a and c). Mathematical calculation of synergy using the Loewe algorithm confirmed enhancement of the cytotoxic action of CMA and venetoclax when used in combination, as evidenced by the positive synergy index values, which correspond to the red range of the heatmaps (Fig. 7, b and d).

Thus, we showed that combination of the genotoxic chemotherapeutic drugs doxorubicin and cisplatin with CMA causes a decrease in their cytotoxic effect on human myeloid leukemia cells, whereas the combined use of the Bcl-2 inhibitor venetoclax with CMA enhances antitumor activity of this therapeutic agent against AML cells.

DISCUSSION

CMA is considered a STING agonist in murine cells [19]. However, its ability to activate human STING has not been demonstrated to date, since CMA is believed to interact poorly with the ligand-binding domain of the human STING, which differs in structure from the murine one [19]. The aim of this work was to study the effect of CMA on human cancer cells. Since our bioinformatic analysis revealed association of the expression of the factors STING and IRF3 with the survival of AML patients (Fig. 2, e and g), as well as pronounced increase in the *STING* mRNA

level in the AML samples compared to the samples from healthy donors (Fig. 2a), we chose the human myeloid leukemia cell lines KG-1 and K562 as model cell lines. These cell lines, like other tumor cells of hematopoietic origin, are characterized by the comparatively high expression level of the genes participating in the STING signaling cascade (Fig. 2, f and h). When analyzing basal expression level of the genes *STING*, *TBK1*, *IRF3*, and *IRF7* in KG-1 and K562 cells, it was found that in the KG-1 line the basal levels of *STING*, *TBK1*, and *IRF7* expression are higher, while in K562 cells higher expression of the *IRF3* gene is observed (Fig. 3). However, upon treatment of the cells with CMA, more pronounced transcriptional response and increase in expression of the *STING*, *TBK1*, *IRF3*, and *IRF7* genes were observed precisely in K562 cells, whereas in KG-1 cells only a comparatively small increase in the *IRF7* expression was detected, while expression of other genes did not change (Fig. 4, a and b). Moreover, in K562 cells, expression of the interferon *IFNB1* and the interleukins *IL1B* and *IL6* increases with increasing CMA concentration (Fig. 4, b and d), whereas in KG-1 cells the response to CMA exposure is less pronounced and limited to the *IFNB1* and *IL6* genes (Fig. 4, a and c). The increased level of the STING cascade activation in K562 cells in response to CMA treatment is also confirmed by the ELISA results showing a more pronounced increase of the IL-6 concentration in K562 cells compared to KG-1 cells. This result is consistent with the previously reported results demonstrating that high level of the cGAS-STING signaling pathway proteins in tumor cells does not always determine functionality of this molecular pathway: in particular, its activity could be suppressed by the oncogenesis-associated mechanisms, including the JAK2/STAT3-dependent regulation [31].

When studying the effect of CMA on human myeloid leukemia cells, we showed that this drug affects not only expression of the STING-dependent type I interferons and pro-inflammatory cytokines but also changes expression profile of the apoptotic factors. In K562 cells, CMA caused a more pronounced increase in the expression of the genes involved in regulation of mitochondrial apoptosis, including *BAK1* (BAK), *BBC3* (PUMA), *BAX*, *BAD*, *NOXA*, *BCL2* (Bcl-2), *BCL-XL*, and *MCL1* (Fig. 5d). In KG-1 cells, this effect was weaker, and the most noticeable change at high CMA concentration was shown for the anti-apoptotic gene *BCL2*, which is consistent with the higher resistance of this cell line to the action of CMA (Fig. 5, a and b). Nevertheless, the pattern of changes in the levels of the proteins Bax and Bcl-2 upon CMA treatment was identical for both cell lines: expression of the pro-apoptotic protein Bax increased maximally at the lowest concentration (1 mM) and decreased with increasing dose, whereas expression of the anti-apoptotic factor Bcl-2 increased with increasing CMA concentration (Fig. 5, e and f). Indeed, it has been repeatedly reported by us and other researchers that the level of STING signaling activation could determine its "switch" from the inflammatory response to the triggering of apoptosis [5, 6, 32, 33].

As a result of studying the combined action of CMA and various groups of antitumor drugs on KG-1 and K562 cells, we showed that CMA treatment in combination with doxorubicin and with cisplatin was accompanied by the decrease in the cytotoxic effect of these drugs, whereas the combination with venetoclax, on the contrary, caused a pronounced synergistic effect in both studied lines (Figs. 6 and 7).

Antagonistic action of CMA in combination with doxorubicin and cisplatin is consistent with the increase in the level of the anti-apoptotic factor Bcl-2, both at the mRNA level and at the protein level, in response to treatment with high CMA concentrations. On the other hand, combination of CMA and the Bcl-2 inhibitor venetoclax exerts a synergistic effect on both cell models, which additionally confirms the assumption of the STING-dependent regulation of Bcl-2. We hypothesize that it is precisely under conditions of the Bcl-2-dependent "survival–death" balance determining the fate of the cell that inhibition of Bcl-2 by venetoclax causes a shift of this balance toward the mitochondrial pathway of apoptosis.

Antagonistic action of CMA in combination with doxorubicin and cisplatin is also consistent with the data indicating that in certain types of tumor cells the STING-dependent pro-inflammatory response could promote their adaptation to genotoxic stress. In particular, it has been shown that activation of the STING signaling and pro-inflammatory cytokine response are associated with acquisition of the resistance of human lung cancer cells to tyrosine kinase inhibitors [34]. It has also been demonstrated that the use of the STING agonist ADU-S100 increases resistance of the tumor cells to cisplatin through the NF-κB-dependent mechanism [34].

Since 1995, CMA has been a registered drug in the Russian Federation, belonging to the group of immunostimulants, and it is currently included in the Russian list of essential and vital medicines (Order of the Government of the Russian Federation of December 18, 2025, no. 3867-r). Nevertheless, it should be classified as a drug with unproven efficacy and safety, since independent randomized clinical trials of this drug have not been conducted [35]. Several Russian-language publications report the ability of CMA derivatives to induce production of the type I and II interferons in adults and children [36-38]; however, molecular mechanisms of the interferon-stimulating effect of CMA remain uncharacterized.

Notably, CMA and its derivatives are not included in the WHO recommendations, are not used as immunostimulants in the EU countries and the USA, and are registered only in Russia, Belarus, Ukraine, Kazakhstan, Armenia, and Azerbaijan. In this study, we demonstrated that CMA treatment increases the expression of STING pathway components and genes encoding STING-associated inflammatory mediators in human myeloid leukemia cells (Fig. 4, b and d). Moreover, according to our data, CMA modulates response of the cells to antitumor therapy and could exert either an antagonistic effect (with genotoxic drugs) or a synergistic one (with venetoclax) (Figs. 6 and 7). It should be emphasized that these effects were observed when using CMA in the concentration range of 1-12 mM. However, the results of a pharmacokinetic study of meglumine acridone acetate demonstrate that the maximum concentration after a single intramuscular administration of 500 mg of this drug to the healthy volunteers is reached within 40 min and amounts to 522.0×10^{-5} mg/ml (~20.6 μM) in blood plasma and 554.0×10^{-5} mg/ml (~21.9 μM) in blood serum, which is more than two orders of magnitude lower than the minimal concentrations causing the STING-dependent interferon response in the cell models.

The revealed synergistic action of CMA and the Bcl-2 inhibitor venetoclax is of interest from the standpoint of using CMA to study the mechanisms of switching of the STING signaling from the pro-inflammatory to the pro-apoptotic program in human myeloid leukemia cells, since venetoclax is one of the most frequently prescribed targeted drugs for the treatment of myeloid leukemia. However, the high concentrations of CMA required for activity, unattainable in patients' plasma, preclude its consideration as a potentially applicable component of combination therapy.

Thus, our study demonstrates that CMA could be considered a stimulator of the STING signaling cascade under experimental conditions. However, the clinical use of CMA requires further substantiation through rigorous preclinical and clinical studies of its molecular mechanism of action and immunostimulatory effects at therapeutically achievable concentrations.

CONCLUSION

In this work, it was shown that the STING signaling cascade has potential functional and prognostic significance in the human myeloid leukemia. Bioinformatic analysis revealed increased *STING* expression in the AML samples and association of its high expression level with the less favorable prognosis, whereas high levels of *IRF3* correlate with better patient survival. These data point to the ambiguous role of the individual components of the STING signaling cascade in myeloid malignancies.

Using the KG-1 and K562 cell models, it was established that, despite the higher expression of *STING*, *TBK1*, and *IRF7* in KG-1 cells, the more pronounced CMA-induced transcriptional response is observed in the K562 cell line, which is characterized by a higher level of IRF3. In both cell lines, CMA not only activates the STING-associated pro-inflammatory response but also alters the expression of genes regulating the mitochondrial apoptotic pathway, with both effects being more pronounced in K562 cells.

The most important result from a therapeutic point of view is demonstration of the multidirectional effect of CMA on the sensitivity of cells to antitumor drugs. The combined use of CMA with doxorubicin and cisplatin reduces their cytotoxic activity, whereas the combination of CMA with the Bcl-2 inhibitor venetoclax leads to the pronounced synergistic effect in both studied myeloid leukemia cell lines. Thus, CMA should be considered a context-dependent modulator of the STING signaling pathway. Taking into account the previously demonstrated species-specificity of the CMA effects and high *in vitro* concentrations required for the induction of the STING-associated response in human cells, further studies are needed aimed at determining the exact molecular mechanism of action of CMA, its immunostimulating potential, and the prospects of combining it with Bcl-2 inhibitors for treatment of myeloid leukemia.

Abbreviations

AML	acute myeloid leukemia
CMA	acridone acetic acid
ELISA	enzyme-linked immunosorbent assay
ER	endoplasmic reticulum
IC50	half-maximal inhibitory concentration
mRNA	messenger ribonucleic acid
MTT	3-(4,5-dimethylthiazol-2-yl)-2,5-diphenyltetrazolium bromide
PAGE	polyacrylamide gel electrophoresis
RPMI	Roswell Park Memorial Institute

Supplementary information

The online version contains supplementary material available at https://doi.org/10.1134/S0006297926601772.

Contributions

A. A. Daks and I. A. Nevzorov – concept and supervision of the work; P. E. Korableva and I. A. Nevzorov – conducting the experiments; P. E. Korableva, I. A. Nevzorov, A. A. Daks, O. Yu. Shuvalov, and S. E. Parfenyev – processing the experimental results and discussing the results of the study; A. A. Daks,

I. A. Nevzorov, and P. E. Korableva – writing the text; A. A. Daks – editing the text of the article.

Funding
This study was financially supported by the Russian Science Foundation (project no. 26-15-00428).

Ethics approval and consent to participate
This work does not contain any studies involving human or animal subjects.

Conflict of interest
The authors declare no conflict of interest.

REFERENCES

1. Larabi, A., et al. (2013) Crystal structure and mechanism of activation of TANK-binding kinase 1, *Cell Rep.*, **3**, 734-746, https://doi.org/10.1016/j.celrep.2013.01.034.
2. Zhang, C., et al. (2019) Structural basis of STING binding with and phosphorylation by TBK1, *Nature*, **567**, 394-398, https://doi.org/10.1038/s41586-019-1000-2.
3. Liu, S., et al. (2015) Phosphorylation of innate immune adaptor proteins MAVS, STING, and TRIF induces IRF3 activation, *Science*, **347**, aaa2630, https://doi.org/10.1126/science.aaa2630.
4. Jing, T., et al. (2020) The structural basis of IRF-3 activation upon phosphorylation, *J. Immunol.*, **205**, 1886-1896, https://doi.org/10.4049/jimmunol.2000026.
5. Korneenko, T. V., et al. (2023) At the crossroads of the cGAS-cGAMP-STING pathway and the DNA damage response: implications for cancer progression and treatment, *Pharmaceuticals*, **16**, 1675, https://doi.org/10.3390/ph16121675.
6. Nevzorov, I. A., et al. (2026) Methyltransferase SETD7 as a regulator of STING-dependent cytokine response in lung cancer cells, *Int. J. Mol. Sci.*, **27**, 4020, https://doi.org/10.3390/ijms27094020.
7. Ishikawa, H., et al. (2009) STING regulates intracellular DNA-mediated, type I interferon-dependent innate immunity, *Nature*, **461**, 788-792, https://doi.org/10.1038/nature08476.
8. Yi, G., et al. (2016) Hepatitis C virus NS4B can suppress STING accumulation to evade innate immune responses, *J. Virol.*, **90**, 254-265, https://doi.org/10.1128/JVI.01720-15.
9. Wu, J.-J., et al. (2015) Inhibition of cGAS DNA sensing by a herpesvirus virion protein, *Cell Host Microbe*, **18**, 333-344, https://doi.org/10.1016/j.chom.2015.07.015.
10. Li, Y., et al. (2017) Regulating STING in health and disease, *J. Inflamm.*, **14**, 11, https://doi.org/10.1186/s12950-017-0159-2.
11. Feng, Q., et al. (2024) cGAS-STING pathway in systemic lupus erythematosus: biological implications and therapeutic opportunities, *Immunol. Res.*, **72**, 1207-1216, https://doi.org/10.1007/s12026-024-09525-1.
12. Pokatayev, V., et al. (2016) RNase H2 catalytic core Aicardi-Goutières syndrome-related mutant invokes cGAS-STING innate immune-sensing pathway in mice, *J. Exp. Med.*, **213**, 329-336, https://doi.org/10.1084/jem.20151464.
13. Deng, L., et al. (2014) STING-dependent cytosolic DNA sensing promotes radiation-induced type I interferon-dependent antitumor immunity in immunogenic tumors, *Immunity*, **41**, 843-852, https://doi.org/10.1016/j.immuni.2014.10.019.
14. Shen, M., et al. (2025) The cGAS-STING pathway in cancer immunity: mechanisms, challenges, and therapeutic implications, *J. Hematol. Oncol.*, **18**, 40, https://doi.org/10.1186/s13045-025-01691-5.
15. Falahat, R., et al. (2021) Epigenetic reprogramming of tumor cell-intrinsic STING function sculpts antigenicity and T cell recognition of melanoma, *Proc. Natl. Acad. Sci. USA*, **118**, e2013598118, https://doi.org/10.1073/pnas.2013598118.
16. Xia, L., et al. (2025) Mitochondrial DNA-activated cGAS-STING pathway in cancer: mechanisms and therapeutic implications, *Biochim. Biophys. Acta Rev. Cancer*, **1880**, 189249, https://doi.org/10.1016/j.bbcan.2024.189249.
17. Kramer, M., et al. (1976) Antiviral activity of 10-carboxymethyl-9-acridanone, *Antimicrob. Agents Chemother.*, **9**, 233-238, https://doi.org/10.1128/AAC.9.2.233.
18. Taylor, J. L., et al. (1980) High-yield interferon induction by 10-carboxymethyl-9-acridanone in mice and hamsters, *Antimicrob. Agents Chemother.*, **18**, 20-26, https://doi.org/10.1128/AAC.18.1.20.
19. Cavlar, T., et al. (2013) Species-specific detection of the antiviral small-molecule compound CMA by STING, *EMBO J.*, **32**, 1440-1450, https://doi.org/10.1038/emboj.2013.86.
20. Bartha, Á., et al. (2021) TNMplot.com: a web tool for the comparison of gene expression in normal, tumor and metastatic tissues, *Int. J. Mol. Sci.*, **22**, 2622, https://doi.org/10.3390/ijms22052622.
21. Tang, Z., et al. (2017) GEPIA: a web server for cancer and normal gene expression profiling and interactive analyses, *Nucleic Acids Res.*, **45**, W98-W102, https://doi.org/10.1093/nar/gkx247.
22. Győrffy, B., et al. (2013) Online survival analysis software to assess the prognostic value of biomarkers using transcriptomic data in non-small-cell lung cancer, *PLoS One*, **8**, e82241, https://doi.org/10.1371/journal.pone.0082241.

23. Jin, H., et al. (2023) Systematic transcriptional analysis of human cell lines for gene expression landscape and tumor representation, *Nat. Commun.*, **14**, 5417, https://doi.org/10.1038/s41467-023-41132-w.
24. Ianevski, A., et al. (2022) SynergyFinder 3.0: an interactive analysis and consensus interpretation of multi-drug synergies across multiple samples, *Nucleic Acids Res.*, **50**, W739-W743, https://doi.org/10.1093/nar/gkac382.
25. Samson, N., et al. (2022) The cGAS-STING pathway and cancer, *Nat. Cancer*, **3**, 1452-1463, https://doi.org/10.1038/s43018-022-00468-w.
26. Barber, G. N. (2015) STING: infection, inflammation and cancer, *Nat. Rev. Immunol.*, **15**, 760-770, https://doi.org/10.1038/nri3921.
27. Zhang, Z., et al. (2025) The role and mechanism of the cGAS-STING pathway-mediated ROS in apoptosis and ferroptosis induced by manganese exposure, *Redox Biol.*, **85**, 103761, https://doi.org/10.1016/j.redox.2025.103761.
28. Tewey, K., et al. (1984) Adriamycin-induced DNA damage mediated by mammalian DNA topoisomerase II, *Science*, **226**, 466-468, https://doi.org/10.1126/science.6093249.
29. Rosenberg, B., et al. (1969) Platinum compounds: a new class of potent antitumour agents, *Nature*, **222**, 385-386, https://doi.org/10.1038/222385a0.
30. Souers, A. J., et al. (2013) ABT-199, a potent and selective BCL-2 inhibitor, achieves antitumor activity while sparing platelets, *Nat. Med.*, **19**, 202-208, https://doi.org/10.1038/nm.3048.
31. Suter, M. A., et al. (2021) cGAS-STING cytosolic DNA sensing pathway is suppressed by JAK2-STAT3 in tumor cells, *Sci. Rep.*, **11**, 7243, https://doi.org/10.1038/s41598-021-86644-x.
32. Gulen, M. F., et al. (2017) Signalling strength determines proapoptotic functions of STING, *Nat. Commun.*, **8**, 427, https://doi.org/10.1038/s41467-017-00573-w.
33. Korableva, P. E., et al. (2024) Activation of the STING-mediated signaling pathway in human tumor cells under the action of acridoneacetic acid, in *Proc. III Int. Sci. Pract. Conf. Student Sci. Soc. St. Petersburg State Univ.*, St. Petersburg.
34. Lv, Q.-M., et al. (2023) Cancer cell-autonomous cGAS-STING response confers drug resistance, *Cell Chem. Biol.*, **30**, 591-605.e4, https://doi.org/10.1016/j.chembiol.2023.05.005.
35. Spirin, A. A. (2026) *Improving the Quality of Functioning of the Contract System in the Procurement Sphere*, PhD Thesis (Economics), St. Petersburg State University of Economics, St. Petersburg.
36. Kovalenko, A., et al. (2014) Interferon-inducing activity and interferon production under the influence of acridoneacetic acid salts [in Russian], *Exp. Clin. Pharmacol.*, **77**, 16-19.
37. Sukhanov, D. S., et al. (2012) Dose-dependent interferon-inducing activity and pharmacokinetics of cycloferon in healthy individuals [in Russian], *Exp. Clin. Pharmacol.*, **75**, 23-26.
38. Shuldyakov, A. A., et al. (2019) Derivatives of acridone acetic acid in pediatric practice [in Russian], *Russ. Bull. Perinatol. Pediatrics*, **64**, 110-116, https://doi.org/10.21508/1027-4065-2019-64-2-110-116.

Publisher's Note. Pleiades Publishing remains neutral with regard to jurisdictional claims in published maps and institutional affiliations. AI tools may have been used in the translation or editing of this article.